ACOUSTIC IMAGING AND IMAGE PROCESSING BY WAVEFRONT RECONSTRUCTION TECHNIQUES

K. Lakin
University of Southern California
Los Angeles, California 90007

ABSTRACT

Acoustic imaging may be accomplished by a process involving the measurement of the amplitude and phase of the wavefront at a remote region and then the reconstruction, using mathematical techniques, of the fields at or near the scattering region. Since the system is coherent, both amplitude and phase images may be obtained. The current system under study employs pulsed CW tone bursts in order to reduce stray echo problems, with quadrature phase detection followed by a digital hardware processor for implementing the reconstruction algorithm. Finally, the image is processed for display and analysis.

INTRODUCTION

The objective of this task is to study acoustic image processing and to implement a pulsed CW imaging system as an extension of the work done previously on the amplitude and phase contrast imaging of transducer near and far field radiation patterns. In that work the precision of the imaging process using CW excitation suggested that the method might well be applied to the problem of defect imaging if the same degree of accuracy could be achieved when the system was used in the pulsed mode. The pulsed mode of operation should be a requirement if real flaws in solids were to be imaged instead of simple objects in water. In the CW system, the overall accuracy was obtained because of the large dynamic range of the network analyzer and its narrow-band, high-resolution phase detection capability. In addition, by using a synthetic array approach, i.e., scanning a 64 x 64 grid using a single transducer, all elements of the array were assured to be identical in response. However, the system was not convenient in terms of data throughput and image processing speed. In addition, the CW mode of operation allows multiple reflections to obscure the desired data, a severe problem in defect imaging where the scattering from front surfaces (such as water-solid) is much stronger than scattered signals coming from the defect located within the solid.

In order to clarify the overall project, we will first discuss the theoretical basis of this particular imaging approach, then describe the previous implementation and its results, next the proposed system will be described, and then the procedure for implementation and progress to date.

Theoretical Approach

The basis of the imaging system, Fig. 1, starts from Huygens theory describing the superposition of a radiation field from many point sources of the source or scattered field[1]

$$UM(u,v) = \frac{2\pi}{jk}\int_{-\infty}^{\infty}\int U(x,y)\,\frac{e^{ikr}}{r}\,dxdy \qquad (1)$$

where UM(u,v) is the measured field in the u,v plane located a distance R from an assumed scattering plane, K is the wavenumber, U(x,y) the source or scattered field, and r is the distance between a scattering element and field position,

$$r = R\left[1 + \frac{1}{R^2}\left((x-u)^2 + (y-v)^2\right)\right]^{\frac{1}{2}}. \qquad (2)$$

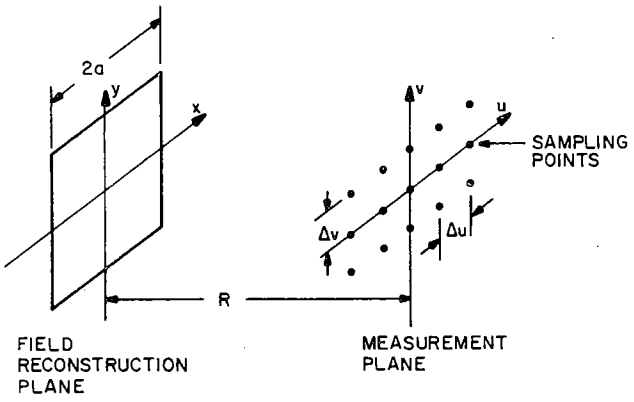

Fig. 1. Reconstruction coordinate system

Using the small angle approximation, we essentially restrict the transverse dimensions of the scattering region and measurement plane such that they are much less than R the distance between planes. In practice, this para-axial approximation restricts the maximum angle between r and R to approximately 30 degrees. However, for the usual cases of water-solid interfaces, this represents a more than adequate angle of incidence due to longitudinal wave cutoff conditions.

Using the para-axial ray approximation, the distance r is approximated by

$$r \approx R + \frac{1}{2R}\left[(x-u)^2 + (y-v)^2\right] \qquad (3)$$

and (1) becomes

$$U(u,v) = 2\pi\frac{e^{ikR}}{ikR}\int\int U(x,y)\exp i\left(\frac{k}{2R}\right)\left[(x-u)^2 + (y-v)^2\right]dxdy \qquad (4)$$

The quadratic phase factor may now be expanded and a normalized relationship is obtained

$$\overline{UM}(u',v') = C\iint\overline{U}(x',y')\ \exp -ik'(u'x'+v'y')\cdot dx'dy' \quad (5)$$

where

$$\overline{UM}(u',v') = U(u',v')\exp -ik'(u'^2+v'^2)/2 \quad (6)$$

$$U(x',y') = \overline{U}(x',y')\exp -ik'(x'^2+y'^2)/2 \quad (7)$$

$$C = 2\pi a^2\,\frac{e^{ikR}}{ikR} \quad (8a)$$

$$x' = x/a \quad (8b)$$

$$y' = y/a \quad (8c)$$

$$u' = u/a \quad (8d)$$

$$v' = v/a \quad (8e)$$

$$k' = \frac{ka^2}{R} = 2\pi(a/\lambda)^2/(R/\lambda) \quad (8f)$$

$$\text{or } k' = \frac{\pi a}{\Delta s} \quad (8g)$$

where $\Delta s = \frac{R\lambda}{2a}$ maximum sampling internal allowed without considerable information loss. At the widest angle of operation, R/a would have a minimum value of $\sqrt{3}$ and the maximum allowed sampling interval would be $\Delta s = (\sqrt{3}/2)\lambda$.

The image processing starts by processing the measured data by first multiplying UM(u',v') by a weighting function which accounts for the fact that the measuring plane actually contains less than the entire energy of the scattered fields. Clearly, small defects or sharp edges of defects such as crack tips scatter widely, and a truncation of the fields due to finite spatial sampling causes a smoothing in the image. The weighting function is used to eliminate the Gibb's ringing created by this artificial truncation. Other image processing will be detailed later.

The smoothed data may now be normalized by effectively removing the parabolic phase, as in (6), which now places the data in the format of a two-dimensional Fourier transform, (5). By taking the inverse transform of (5) we obtain

$$\overline{U}(x',y') = C'\iint UM(u',v')\exp +ik'(u'x',v'y')\cdot du'dv' \quad (9)$$

which is the normalized image field. If phase information is desired, then the parabolic phase unnormalization is carried out, (7). Note that the plane of reconstruction is determined by the parabolic phase normalization and that many images may be formed from one set of measured data.

The concept of superposition implies other useful image processing techniques. For example, since the fields UM(u,v) are made up of a sum of scatter contributions, known scatter fields may be subtracted from the total measured field to yield the field due to a small defect alone. An "aperture stop" may be effectively implemented by numerically weighting the measuring data in an appropriate manner. For example, the central fields could be zeroed or allowed to drive the receiver non-linear in order to gain more dynamic range for the edge fields which define small objects.

Since the imaging technique has its roots in conventional optics, many processing techniques employed there may be usefully employed with the added advantage of having phase and amplitude as variables and not just intensity.

The imaging process may now be summarized: 1) measure the amplitude and phase UM in the measurement plane, 2) weight the fields and correct for known measurement errors such as array non-uniformities, 3) choose a reconstruction plane and phase normalize the measured fields, 4) do a two-dimensional Fourier transform to obtain the normalized scattered fields, and 5) phase unnormalize to obtain the complete fields. This data is now ready for display and possible enhancement.

CW Imaging System

The imaging system shown in Fig. 2 was employed in the study of transducer fields reported in last year's final report. The system is briefly described here in order to set the stage for the system currently under study. The system in Fig. 2 used, almost entirely, "off-the-shelf" laboratory components. The major components include 1) the Tektronix 4051 Graphics System which is basically a desk top calculator with limited graphic capability, 2) a numerically controlled x,y stage to position the transducer in the measurement plane, 3) a network analyzer to measure the magnitude and phase of the transducer signal, 4) digital voltmeters to perform the A/D conversion of the network analyzer results, 5) frequency synthesizer for stable frequency control, and finally 6) an IEEE 488 instrumentation bus to tie all components together under control of the Tektronix 4051.

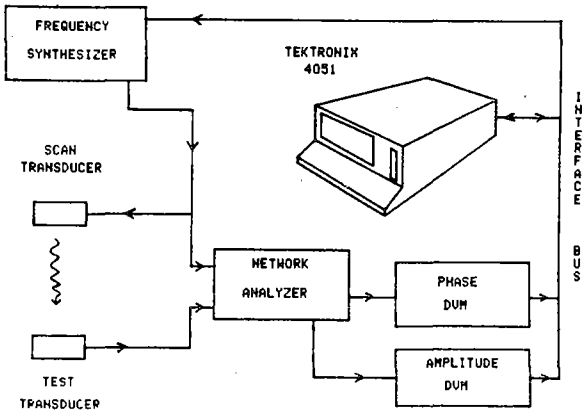

Fig. 2. CW imaging system.

The resultant data was stored on magnetic tape one scan row at a time because of limited memory, and then sent over a 2400 baud RS232C line to a PDP-10 computer. Here the necessary image processing was performed and the image data sent to USC's Image Processing Institute for display, or to a perspective plot subroutine and then back to the 4051 for display and recording. Representative results of the system are shown in Figs. 3a, 3b, and 3c as perspective amplitude and phase plots and as grey scale amplitude respectively.

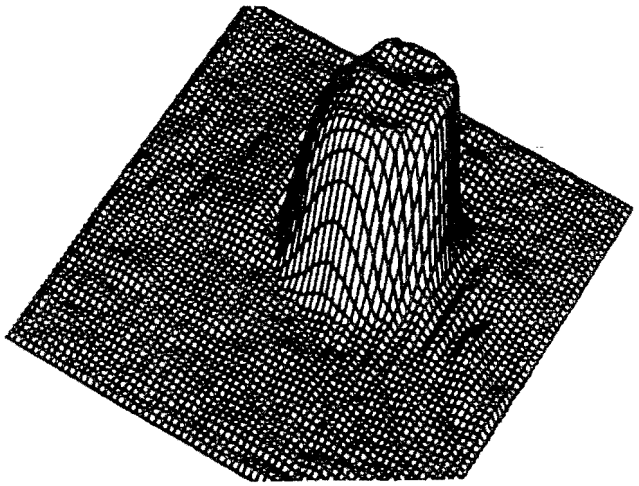

(a)

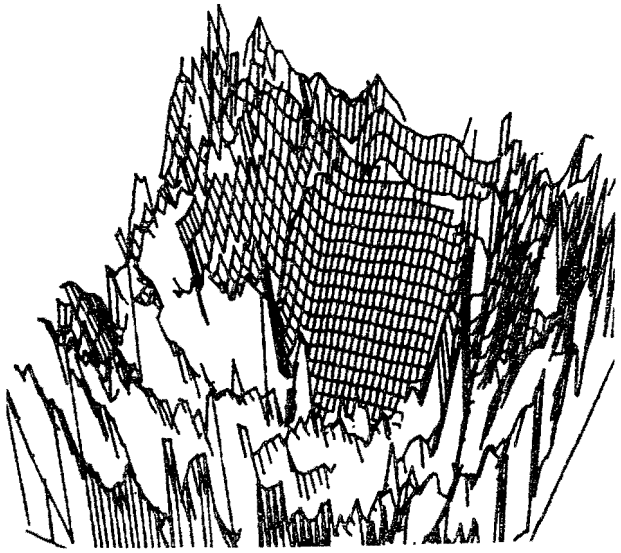

(b)

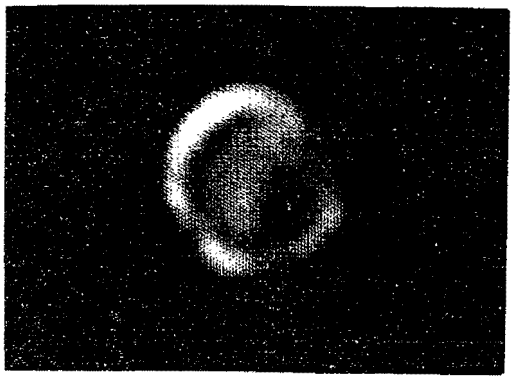

Fig. 3. Reconstructed transducer near field
(a) amplitude
(b) phase
(c) grey scale of amplitude

Whereas the imaging results are very favorable, the system through-put was agonizingly slow for any real imaging system or an imaging study requiring many image formations. The data acquisition time alone was 3-4 hours, due to limitations in the phase measurement caused by mechanical vibrations induced by the stepping motors on the x,y table. In addition, the DVM's were limited in through-put to one reading per second. Data transfer times to the PDP-10 were upward of one hour, due to the inability of the system to accept sustained data bursts. However, once having demonstrated the basic imaging process, we can now define what a more practical system might consist of.

Pulsed CW Imaging System

The natural evaluation of the previous imaging system is the system currently under study which duplicates some of the previous one in functional detail. Clearly, the system must work in the pulsed CW or tone burst mode of operation in order to avoid interference from standing waves caused by extraneous reflections. This requires a tone burst transmitter-receiver combination which must accurately measure the magnitude and phase of the radiation field over a dynamic range of 70 dB (12 bits). The system should have a local array processor to handle the image processing in real time once the data has been taken. An ultrasonic array would considerably speed up the data acquisition process, either in the form of a one-dimensional array mechanically scanned or a two-dimensional array electronically scanned. In the latter case, data could be gathered at a rate of 10-100μs per element or 40-400 ms for a 4096 element array assuming a fast 12 bit A/D converter.

The display system need not change from that type used before except that it should be close to the array processor for rapid data transfer.

In order to efficiently implement this study, we have defined a number of subtasks which are ordered in the approximate flow of image data. The description of the various subtasks and their implementation are described below.

IMPLEMENTATION

Pulsed CW Measuring System

The pulsed measuring system consists of an analog region and A/D converters to provide 2's complement data for reduction and display. The analog portion of the system is a super-heterodyne receiver consisting of a front end mixer followed by a high gain 30 MHz IF amplifier having 4 MHz bandwidth, over 100 dB gain and -120 dBm sensitivity. The first mixer takes the nominally 5 MHz signal from the transducer (or array element) and mixes with a 25 MHz carrier to give the 30 MHz IF signal. The output of the IF amplifier is either a 30 MHz pulse or an envelope of the pulse. In our system, the 30 MHz pulse is sent to two double balanced mixers with proper phase shift and mixed with quadrature shifted 30 MHz reference signals. The output of the detectors is then the real and imaginary components of the pulse signals. These base band pulses are then sent to gated sample and hold modules and then to fast 12 bit A/D converters and then to memory via the IEEE 488 interface bus. Because the analog portion of the system uses the super-heterodyne principle, the input signals may be pulses as well as tone bursts. The generation of the transmit signal also uses the heterodyne principle in order to maintain phase coherence between pulses. The analog and digital positions of the receiver have been completed and are now being calibrated.

Array Design

An array to be used for a holographic imaging system has somewhat different requirements than those used for focused imaging. The holographic transducer array may be constructed with elements more widely spaced than those used for focused beams, the elements are sampled in sequence rather than simultaneously, and the requirements for cross talk in the array are probably somewhat more severe than in focused beam arrays. The more widely spaced array elements make the array construction somewhat more tractable and the sequential access should make the electronics less costly since 2N electronic elements are required for an array of size NxN, rather than N squared similar circuits. Several array designs have been considered with an emphasis placed upon the compatibility of acoustical design and electronic scanning. In general, the array of interest is of size 64x64 with an element spacing of 8 wavelengths, and an operating frequency of 5 MHz. Since the holographic system uses coherent tone burst for measurement, the transducer elements need not be as heavily damped as those used for focused beam A scan. It is hoped that the easing of the damping requirement alone will make the array construction more practical and the elements more uniform and reliable.

Some effort has been directed toward a study of potential array configurations that could be usefully employed in this imaging system. Currently we are looking at arrays that might be used for transmitting only, since the sequential accessing of such elements seems more appropriate to conventional digital circuits. Both array element construction and multiplexing methods are being considered. It is clear that an in-depth study of new array concepts and actual array construction are not within the financial constraints of the current program. However, the initial study has turned up some preliminary useful results.

Acoustic Image Processing

In order to form an image from the acoustic signals, the data must first be cast into a format that allows the inversion to be done with Fourier transform methods. Initially, the data must be windowed to prevent image ringing due to the truncation of the transform and then the parabolic phase factor must be subtracted from the total phase. The formalism may also be recast into the form of a double convolution as shown in (10) for the continuum and in (11) for the discrete case.

$$U(x',y')=\int\int UM(u',v')F(y'-v')F(x'-u')dv'du' \tag{10}$$

$$U_{IJ} = \sum_{KL}\sum UM_{KL}\, F_{JL}\, F_{IK} \tag{11}$$

$$\text{where } F(z) = \exp(-ik'z^2) \tag{12}$$

Clearly, with the parabolic phase factored in, the problem is one of convolving the circular functions with the field data. For the case of a 64x64 data set, 4096 complex multiplications are required for each of the 64 rows and the process is repeated for each of the 64 columns for a total of over 500,000 complex multiplications. Accordingly, we are planning to use hardware multipliers to do the complex arithmetic and directly cycle the data to the multipliers transparent to the microprocessor. In this manner, we can achieve a good compromise between hardware cost and computational time, since memory is relatively inexpensive and the hardware multipliers are less than $200 each, and multiply in less than 150 ns. Thus by using two multiplications per memory cycle, we can obtain the product of two 12 bit numbers in 300 ns and the two-dimensional convolution in less than 200 ms, which should allow for a near real time display of the transform and a feature for zoom focusing of the image by the operator. In the case of imaging through a water-solid interface, as many as 4096 transforms would be required in the worst case to find the interface fields, but this would take less than 14 seconds. Once having the interface fields, the image within the solid would be obtained in the usual manner in less than 200 ms.

By implementing the FFT in hardware, we could achieve a time compression by a factor of 10, but with somewhat more circuit complexity, since the parabolic phase normalization could not be done with the FFT processor. Implementing the two-dimensional convolution by a succession of FFT operations is more time consuming than doing the FFT directly. Our current effort is to brute force the Fourier transform because of circuit simplicity and the need to do the parabolic phase normalization. In the future we intend to implement the FFT array processor and the phase normalization as separate pieces of hardware. The brute force Fourier transform processor is about 50% completed in hardware construction.

Image Display

For our initial work, the mode of display will be the 8 bit grey scale using black and white with the operator having the option of zoom focus and level slicing (contour plots). Eventually, it will be useful to present the data in the form of perspective plots, as was done in the transducer studies, although this requires a lot of code and processing time if hidden lines are to be blanked out. In the meantime, perspective plots have been generated on the Tektronix 4051 Graphics System directly using recently purchased graphic firmware packages and using software written at USC during the third quarter of the project.

ACKNOWLEDGMENT

This research was sponsored by the Center for Advanced NDE, operated by the Science Center, Rockwell International, for the Defense Advanced Research Projects and the Air Force Materials Laboratory under Contract F33615-74-C-5180.

REFERENCE

1. K.M. Lakin and A. Fedotowsky, "Characterization of NDE Transducers and Scattering Surfaces Using Phase and Amplitude Measurements of Ultrasonic Field Patterns", IEEE Trans. SU-23, No. 5, September 1976.